36th International Electric Vehicle Symposium and Exhibition (EVS36)
Sacramento, California, USA, June 11-14, 2023

Qualitative Comparison of Axial-Field Magnetic-Differential Flux-Reversal Motors with and without Permanent Magnets

Tengbo Yang[1], K. T. Chau[1], Zhichao Hua[1], and Hongliang Pang[1]

[1]*Department of Electrical and Electronic Engineering, The University of Hong Kong, Hong Kong, China, ktchau@eee.hku.hk*

Executive Summary

In this paper, two axial-field flux-reversal motors with magnetic differential application are proposed. One is with permanent magnets, while the other motor has no permanent magnets, namely a DC-excited motor. Having permanent magnets as the magnetic field source takes advantage of high torque, power density, and efficiency. However, it suffers from high costs and the risk of demagnetization. The DC-excited motor can easily avoid such risks and provide a low-cost solution, but its efficiency is downgraded noticeably by the copper loss. Therefore, this paper thoroughly compares the two aforementioned motors to find a more suitable motor for the newly proposed magnetic differential application. Simulation investigation is conducted on their back electromotive force, static torque, flux regulation capability, magnetic force, and efficiency and loss, with simulation results using three-dimensional finite element analysis. The thorough evaluation of the performances of the two proposed motors can provide a guide on the selection of motors given various application scenarios.

Keywords: Permanent magnet, finite element analysis, flux reversal motor, DC-excited motor, magnetic differential.

1 Introduction

In the context of the energy crisis and global warming, the electric vehicle (EV) is now a popular choice for an increasing amount of people as they travel around. Along with the thriving of the EV, the relevant technologies, such as onboard battery and EV charging, etc., have shown a noticeably rapid evolvement with time. A thorough report on state-of-the-art EV batteries and methods of battery management has been provided, with foresight on the move-and-charge systems and wireless power drives [1]. One of the key advantages of the wireless power drive is that the receiver side, which avoids neither the energy storage nor the wired power source, can be more robust and reduce construction and maintenance costs [2].

Besides, the development of EVs is still pushing forwards with more and more advanced machines and propulsion systems. Due to good torque output, high-power density, and the flexible mechanical structure design possibility, the vernier machines have recently gained much attention [3-5]. Considering the PM

configuration, the interior PM vernier machines with different PM arrangements aiming at improving the flux modulation effect were compared with the conventional PM vernier machine [6], which also presented a detailed view of the application of the PM vernier machines for automatic guided vehicles. Owing to the vital advantage of simple rotor structure, the vernier PM machines evolved into doubly salient PM (DSPM) machines, flux reversal PM (FSPM) machines, and flux switching (FSPM) machines, etc., with different PMs and windings configuration [7-10]. For example, the impact of the toroidally-wound configuration for FRPM machines and FSPM machines were investigated, respectively. And the results showed that with an improved pitch factor, short end-winding, and larger effective coil area, the torque output can be boosted [11, 12]. A novel multi-objective optimization framework was proposed to guide the design of radial-axial (RF) hybrid excitation machines for EVs, which not only increases the machine's torque output but also suppresses the torque ripple [13].

Apart from functioning in the EV propulsion system as merely the motors, the machines based on the flux modulation principle can as well be applied to the EV transmission system. The idea of magnetic gears was presented, showing the advantages over mechanical gearboxes while reducing the rare-earth cost [14]. An electromagnetic gear with a changeable gear ratio was introduced to provide better gear ratio controllability and overloading protection [15]. As an essential part of directing the torques to different wheels when the vehicles are cornering, the conventional mechanical differential (MechD) system seems bulky nowadays for EVs. Many attempts are made trying to get rid of the clumsy gear. For example, a torque distribution strategy that optimizes energy efficiency is proposed by utilizing a dynamic programming algorithm for in-wheel motor drives [16]. By directly driving each wheel using individual motors rather than an exact differential gear to decouple wheels on the same axle, the electronic differential (ElecD) system takes advantage of the increasingly fast computational speed of onboard chips. However, the ElecD system requires more numbers of machines to be installed on vehicles [17, 18]. This hurts onboard space utilization and complexifies the control strategies of EVs, which can lead to unexpected control errors and risk the operation of EVs.

Therefore, to spare more onboard space and relax the complicated control strategy of motors, the magnetic differential (MagD) system has been proposed [19, 20]. By skillfully re-designing the windings of the stator-PM motors, the MagD system combines the functions of the motor and differential into one double-rotor motor. In this way, the control of the whole propulsion system can be largely simplified, and the number of needed motors is reduced. Nevertheless, research on the MagD system is quite rare. And given that various types of PM motors have the potential to be modified for MagD application [21] and that there is barely any research on the DC-excited motors for MagD application, it is necessary to find out suitable motor types for MagD application under diverse conditions. Thus, this paper compared two types of motors, namely an axial-flux (AF) double-rotor (DR) FRPM motor and an AF-DR DC-excited FR motor with MagD application, or simply called MagD motors. The purpose is to show that under the same sizing condition, how will having PMs or not impact the motor performances and to provide guidance on the motor choice for different applications. The back electromotive force (EMF), the electromagnetic torque, the flux regulation ability, and the magnetic forces on rotors, as well as the motor efficiency and iron loss, are thoroughly investigated in this paper by three-dimensional (3D) finite element analysis (FEA).

2 Motor topologies and operation principles

2.1 Motor topologies

The topologies of the proposed AF-DR FRPM motor and AF-DR DC-excited FR motor with MagD application are shown in Fig. 1a and Fig. 1b, respectively. As one can see, both motors have their stators sandwiched by the left and right rotors, and both motors have two sets of windings. The three-phase AC currents are injected into the armature windings to rotate the rotors. The differential function of the FRPM MagD motor is realized by artfully positioning the magnetic coupling (MC) windings into the stator. On the other hand, however, the DC-excited FR MagD motor can only rely on the DC windings for both motor and differential functions.

The FRPM one has PMs attached at the surface of its stator to create magnetic flux, and they adopt the NS-SN PM arrangement. As revealed by the name, the DC-excited FR MagD motor generates its magnetic field by the DC windings. The DC-excited one is designed to have a similar magnetic field pattern as the FRPM

counterpart, and Fig. 2 shows the process of adapting the PMs to DC windings. The first step is replacing the PMs with the cooper windings according to Ampere's law and also getting rid of the MC windings. Now the DC windings are in an NS-SN arrangement. The second step is connecting the adjacent windings with the same winding direction. Now, one can see that, although the DC windings are in the arrangement of NS-NS on the stator, however, it can generate a magnetic field similar to the NS-SN PM arrangement. There are merits to the application of the NS-NS DC-winding arrangement, which reduces the amount of copper wire in use. The copper loss is reduced, and the cooling condition is improved due to the shorter winding length. In addition, the total mass is decreased, which benefits the power density and torque density of the motor.

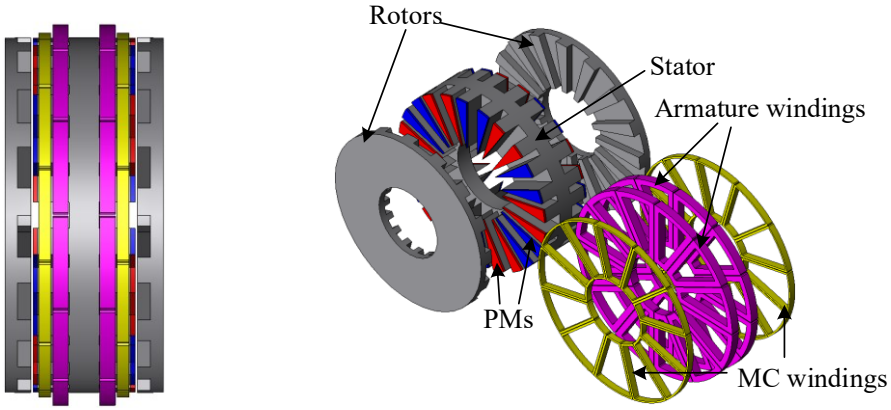

(a)

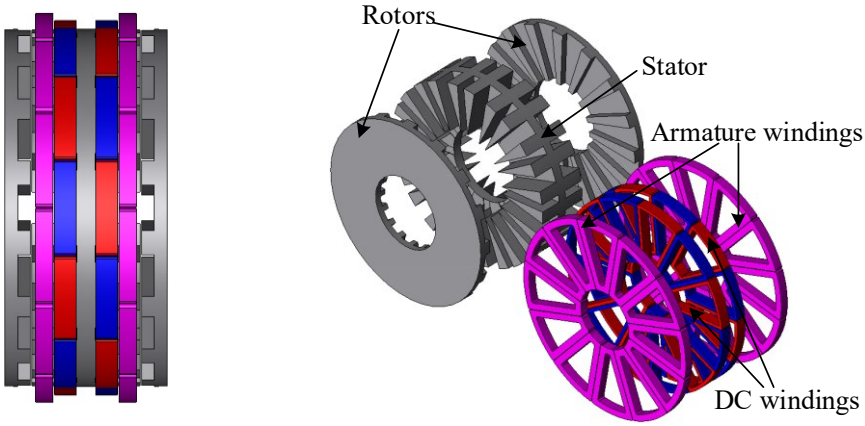

(b)

Figure1: Topologies of the proposed motors with MagD application for EVs. (a) AF-DR FRPM MagD motor. (b) AF-DR DC-excited FR MagD motor.

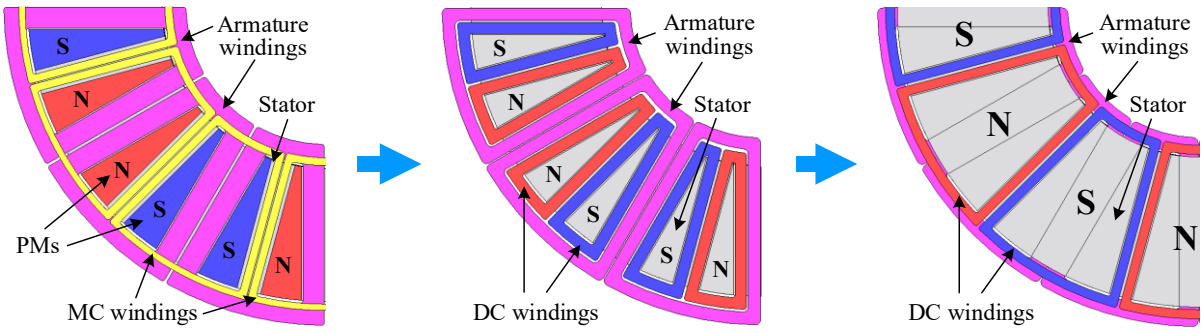

Figure2: Procedures of transforming a FRPM MagD motor into a DC-excited FR MagD motor.

2.2 Operation principles

The operation principle of the FRPM MagD motor is depicted in Fig. 3. One can see that when the vehicle is moving straight, there is only PM flux distributed equally on two rotors. Then, when there is a need for cornering, the MC windings will be activated with DC currents. Therefore, the MC flux will be created. And given the tactful configuration of the MC windings, the MC flux will reversely regulate the PM flux. As shown in Fig. 3, the total flux will be boosted on one side, while on the other side, it will be weakened. Once the vehicle starts to take a turn, the two rotors will be unaligned. The magnetic flux with an unaligned rotor position is also provided in Fig. 3. One can see that no matter the rotor position, the differential function can always be realized by activating the MC windings.

Similarly, as shown in Fig. 4, the operation of the DC-excited FR MagD motor follows the same idea of reversely regulating the flux on two rotors. However, since there is no PM to generate constant PM flux, the DC flux is created by the DC windings. The DC windings will have the same amount of current on the two stator sides when the vehicle moves straightforwardly. And when the vehicle tries to corner, the DC current will be increased on one side of the stator, whereas on the other side, it will be suppressed. Thus, the unequal flux will be seen on the two rotors if the armature windings' current density remains unchanged, the torques provided on the two rotors will be different, and the differential function will be realized. Also, the differential function can likewise be achieved when the rotors are in unaligned positions for the DC-excited FR motor, as demonstrated in Fig. 4.

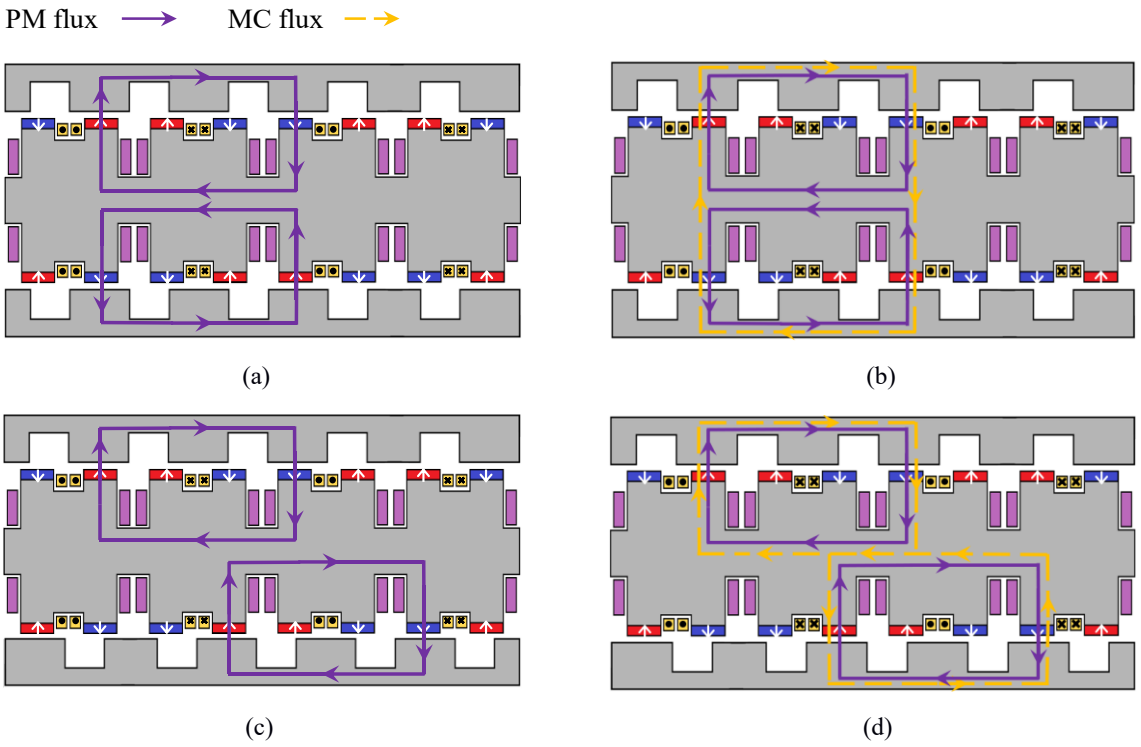

Figure3: Operation principle of FRPM MagD motor [21]. Aligned rotor position: (a) Moving straightforwardly. (b) Cornering. Unaligned rotor position: (c) Moving straightforwardly. (d) Cornering.

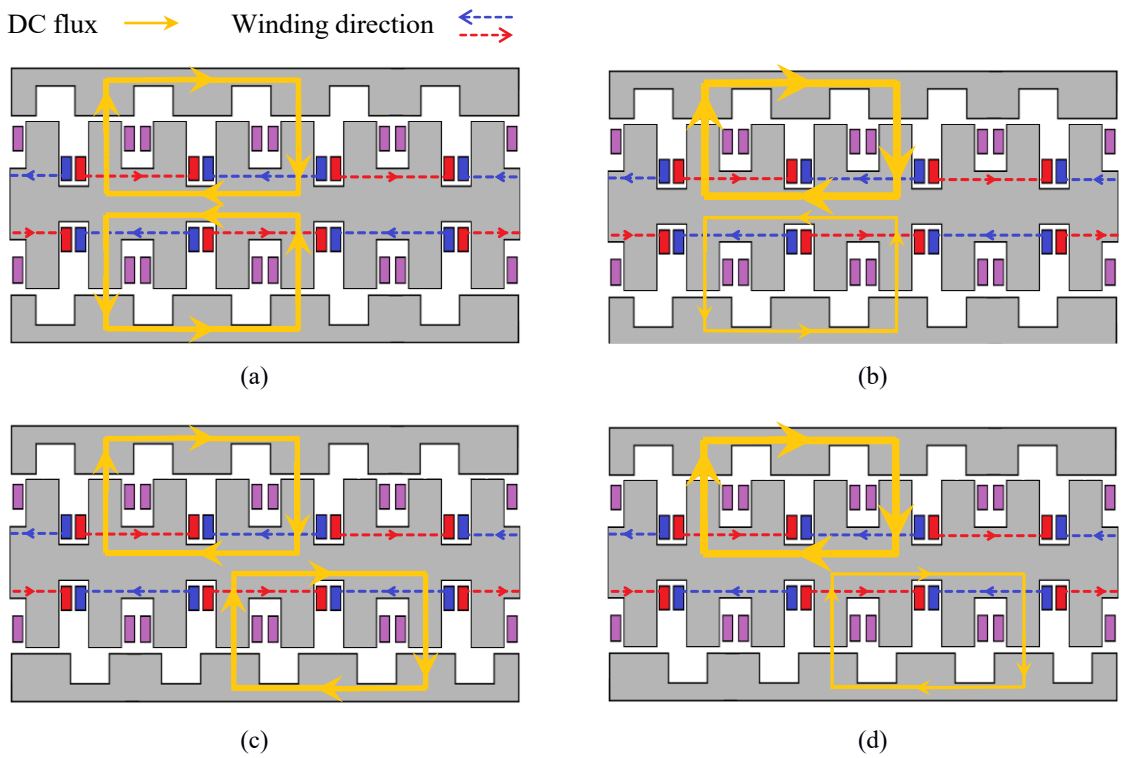

Figure4: Operation principle of DC-excited FR MagD motor. Aligned rotor position: (a) Moving straightforwardly. (b) Cornering. Unaligned rotor position: (c) Moving straightforwardly. (d) Cornering.

3 Structural optimization

The motor design and optimization are conducted using the FEA software JMAG. Before conducting the structural optimization, some constraints for the two MagD motors should be set regarding a reasonable size for EVs. The outer diameter is set to 220 mm, and the stack length of the motors is set to 90 mm. Given the motor size, the air gap is chosen as 1 mm. Considering a natural cooling condition, the armature current density can be 6 A/mm^2. And the filling factor of the windings in the stator slots is empirically set to 0.55. The optimization process of these two motors and the one shown in [21] are alike. Therefore, this paper will follow a similar process of obtaining the optimal structure of the two aforementioned MagD motors. It should be noted that by optimal structure, it means a motor structure providing high torque output or torque density with low torque ripple.

One example of the optimization provided in this paper is the optimization of the split ratio k_{io}. Since one of the objectives is to find a larger output torque, and the k_{io} is a critical parameter to determine the output torque of AF motors, it is reasonable to optimize the k_{io} at the top priority. The split ratio can be written as:

$$k_{io} = D_i / D_o \tag{1}$$

where D_i is the inner stator diameter, and D_o is the outer stator diameter. And the relationship between the k_{io} and the motor output torque T_{out} can be derived as [22]:

$$T_{out} = \frac{\pi}{4} B_a E_L k_d k_{io} (1 - k_{io}^{\ 2}) D_o^{\ 3} \tag{2}$$

where B_a is the air-gap flux density, E_L is the electrical loading, and k_d stands for the distribution factor of armature windings. The simulation results of the torque and the torque ripple are shown in Fig. 5. One can see that when k_{io} is increasing, the torque peaks around k_{io} = 0.5, with its torque ripple monotonically increasing. It should also be mentioned that a larger k_{io} means less motor mass since the total volume of iron and copper materials is reduced. Thus, considering the torque density, the k_{io} is optimized to 0.55 since the

torque density growth after k_{io} = 0.55 slows down. The torque ripple needs to be further reduced by optimizing other structural parameters.

Lots of trade-offs are made between torque, torque density, and also torque ripple during the design of various structural parameters. And finally, some important design parameters for two proposed MagD motors after optimization are listed in Table 1. Each motor turns out to have a relatively large torque, a reduced torque ripple, and a reasonably large torque density, given the size constraints. It is worth pointing out that the application of PM materials can affect motor design in many aspects. For example, the stator yoke of the DC-excited FR MagD motor is thinner than that of its PM counterpart since the magnetic field created by the DC current is not as strong as by the PMs. Therefore, more slot area is needed to accommodate DC windings. And this is also the reason for the DC-excited motor having larger armature winding arc and DC winding arc than the PM motor. On the other hand, however, the DC-excited motor can benefit from the smaller magnetic field that its stator has a lower possibility to saturate compared with the PM one.

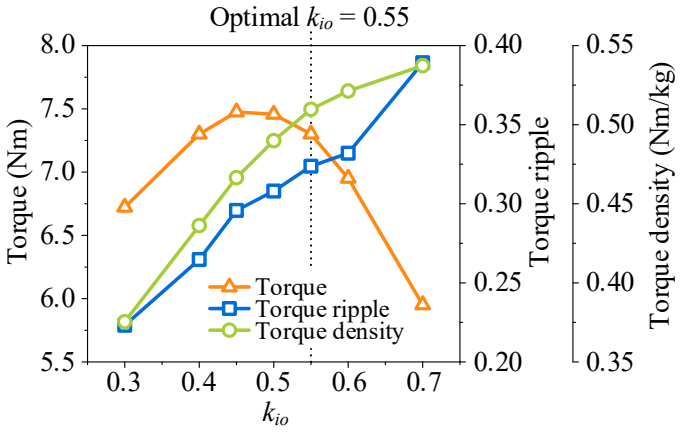

Figure5: Optimization of the split ratio for DC-excited FR MagD motor.

Table 1: Key design parameters of the two MagD machines after optimization

Parameters	PM	DC-excited	Parameters	PM	DC-excited
Outer diameter	220 mm		Armature winding arc	10°	12°
Inner diameter	132 mm	121 mm	MC/DC winding arc	6°	7°
Air-gap length	1 mm		PM thickness	2.5 mm	/
Axial stack length	90 mm		Stator yoke thickness	15 mm	11 mm
Rotor yoke length	6 mm		AC windings turns	38	40
Rotor teeth length	5 mm	8 mm	MC/DC windings turns	20	22
Rotor slot arc	12.0°	14.6°	Slot filling factor	0.55	

4 Performance comparison of two MagD motors

The motor performances are evaluated by the FEA simulation. To assess the performances of these two motors equitably, the evaluating conditions are pre-determined. The rated rotor speed is 900 rpm, and the rated armature current and DC current are both set as 6 A/mm^2 considering an air-cooling condition. In this section, the no-load back-EMFs, the static torques, the flux regulating abilities, the magnetic forces between stator and rotors, as well as the efficiencies and losses of two proposed MagD motors will be investigated, and a thorough comparison will be presented to show their unique characteristics for different applications.

4.1 No-load back-EMF and static torque performances

The no-load back-EMFs of the two motors under rated no-load operation are depicted in Fig. 6. Both motors have a rotor speed of 900 rpm, and the DC current density of the DC-excited motor is 6 A/mm^2. The figure shows that the PM motor has a better back-EMF waveform than the DC-excited one. Firstly, due to the large magnetic field provided by the PM materials, the PM motor has an amplitude nearly twice of its DC-excited counterpart, which is 49.4 V compared to 29.0 V. Besides, the back-EMF waveform of the PM motor looks way more sinusoidal than the one of the DC-excited motor. By calculating the total harmonic distortion (THD), it can be found that the back-EMF THD of the motor with PM is 4.7%, while for the DC-excited motor, the THD of its back-EMF is 9.4%.

The rated loaded operation is also evaluated. The steady torques and cogging torques of the two proposed motors are shown in Fig. 7. These torques are obtained by summing the torques on the left and right rotors together. Similarly, as a result of using PMs, the FRPM MagD motor has a total torque close to twice that of the DC-excited one. Therefore, given a similar torque ripple amplitude, the PM motor can have a relatively lower torque ripple than the DC-excited motor. Moreover, since the two motors have the same sizing constraints, the PM motor will thus have a higher torque density. However, as one can find in Fig. 7, the usage of PMs also leads to a large cogging torque. Whereas for the DC-excited motor, its cogging torque is almost zero.

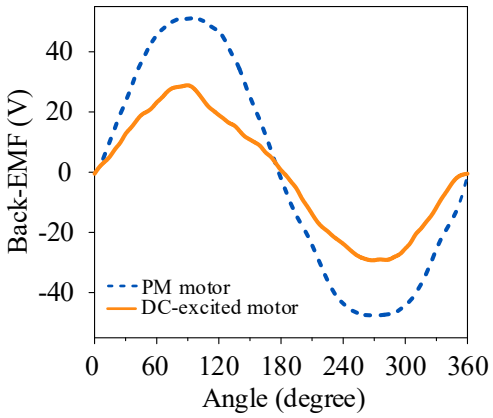

Figure6: No-load back-EMFs of the two proposed MagD motors.

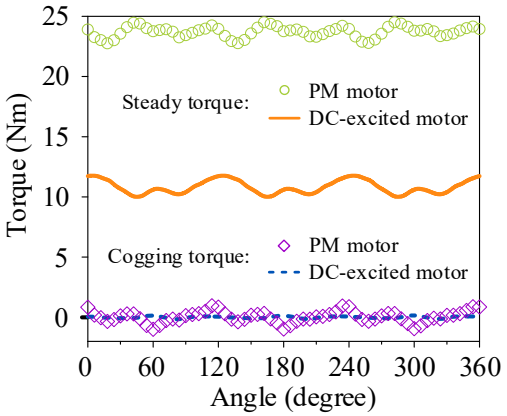

Figure7: Steady torques and cogging torques of the two proposed MagD motors.

4.2 Ability of flux regulation

One major difference between the two MagD motors is the flux regulation ability. Fig. 9 and Fig. 10 show the no-load back-EMFs and static torques of two motors when adopting different MC and DC currents to regulate the flux. For a better understanding of differential function, J_{DC}, the DC-winding current density of the DC-excited motor, is the density for the left-side DC windings. And that on the right-side DC windings equals (7- J_{DC}) A/mm^2. The rated load for the FRPM motor is at a point where the armature current density equals 6 A/mm^2 and no MC current. As for the DC-excited one, its rated load is with the same armature current density as the FRPM one while having a DC current density of 6 A/mm^2 for both left and right sides.

In Section 2, the operation principles show that both motors can regulate the flux, thus varying the back-EMFs and torques. And the simulation results in Fig. 9 and Fig. 10 validate the operation principle. It is no doubt that the FRPM motor has the advantage of high air-gap flux density over its magnetless counterpart due to the PM application. Therefore, at the rated load point, one can see that the FRPM motor has higher amplitudes of no-load back-EMF and static torque than the DC-excited motor. However, judging from the range of back-EMFs and torques under different MC and DC currents, the FRPM motor shows a much weaker ability to regulate the flux compared to the DC-excited motor. This is due to the flux generated by the MC windings being hindered by the constant PM flux, and the surface-mounted PMs increase the equivalent air-gap length on the MC flux path. The total air-gap length for the MC flux equals the physical

air-gap length plus the thickness of the PMs. This largely increases the reluctance on the MC flux path. However, for the DC-excited motor, the air-gap length is exactly the distance between the rotor and stator. Plus, there is not any constant PM flux to affect the magnetic field regulation. Moreover, the MC windings' current density is restricted to avoid the demagnetization of the PM materials, which is never a concern for the DC-excited FR MagD motor. So, it can be concluded that in terms of the flux regulation to realize the differential function, the DC-excited FR MagD motor has a superior advantage over the PM counterpart.

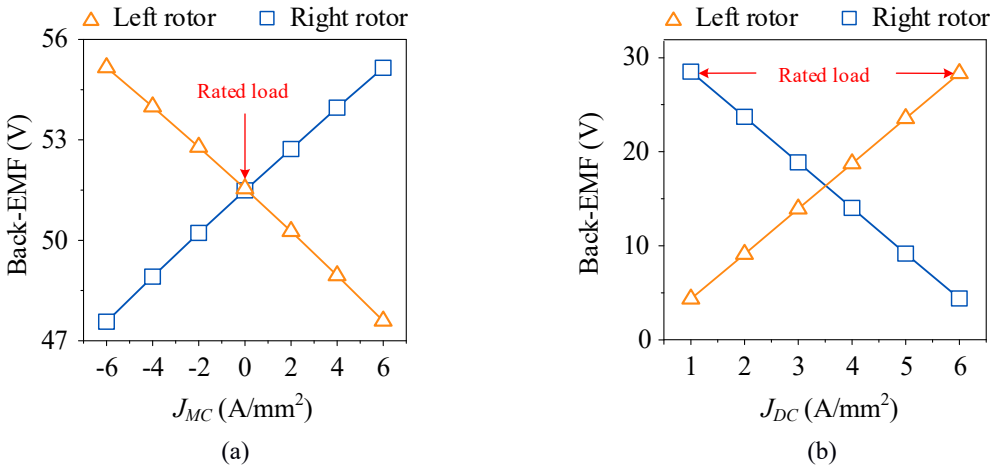

Figure9: No-load back-EMFs under different MC/DC current densities. (a) FRPM MagD motor. (b) DC-excited FR MagD motor.

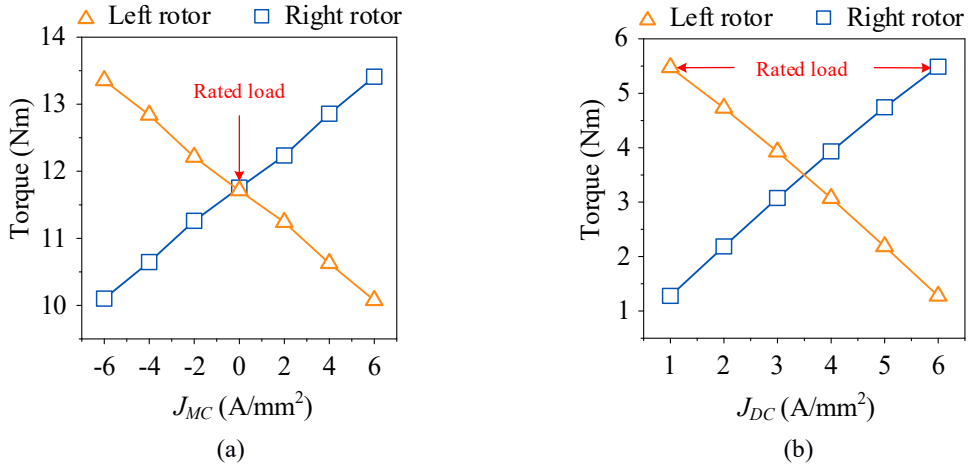

Figure10: Torques under different MC/DC current densities. (a) FRPM MagD motor. (b) DC-excited FR MagD motor.

4.3 Magnetic forces

Another noteworthy difference that this paper would like to discuss is the magnetic forces between the two rotors and their stators for the motors mentioned above. The magnetic forces between the rotors and stators are essential to be tested, which can provide guidance for motor structural mechanisms and manufacturing. An unexpectedly large magnetic force may lead to errors like motor eccentricity, which can risk the operation safety of the motor [23, 24]. The magnetic forces on rotors when they are operating under rated armature current density J_{AC} = 6 A/mm^2 are presented in Fig. 11. Note that in Fig. 11b, the J_{DC} stands for the current density of both left and right DC windings. It can be seen that the FRPM MagD motor has much larger magnetic forces on rotors than the magnetless motor. In addition, the MC flux can weaken or boost such magnetic forces. As for the DC-excited motor, the magnetic forces on its rotors go up with the increase in the absolute value of the DC current density. On the other hand, however, when taking on some load for the PM motor, the magnetic forces slightly rise by nearly 3%, while such forces ramp up to several times of

those in no-load condition for DC-excited FR motor. This means that taking on load can hardly change the magnetic forces on the rotors of the PM motor, but drastic growth can be encountered in the case of the DC-excited motor. But still, even after the magnetic forces significantly increase for the DC-excited motor when on load, the forces are way lower compared with the motor with PMs. In addition, for the J_{DC} that is below zero, it means that the rotors are in reverse spinning direction since the magnetic field is reversed. From Fig. 11b, one can know that the load current can enlarge the magnetic forces when the motor is running forwards. However, when the motor moves backward, such increase will be smaller.

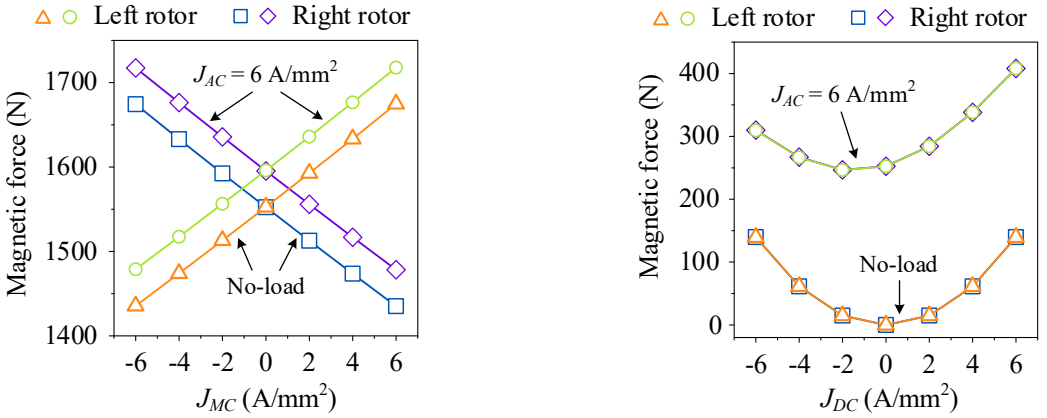

Figure11: Magnetic forces under different MC/DC current densities. (a) FRPM MagD motor. (b) DC-excited FR MagD motor.

4.4 Efficiency and iron loss

Finally, the efficiency and iron loss performances of the two proposed motors are evaluated in a wide range of operation speeds, from 300 rpm to 2100 rpm. The results are separately shown in Fig. 12 and Fig. 13. One can see that the PM motor has a much higher efficiency than the DC-excited counterpart due to the application of PM materials. The DC-excited motor will not only face the problem of the relatively lower torque output but also suffer from the extra copper loss as the result of the DC excitation. Also, as depicted in Fig. 12, one can see that the DC-excited motor works with higher efficiencies when the operation speed is above 1.2 krpm. Nevertheless, the efficiency curve of the PM motor sees a saturation earlier than the DC-excited motor. In Fig. 13, one can see that the DC-excited motor has higher iron loss under the same operation speed, which also hurts its efficiency.

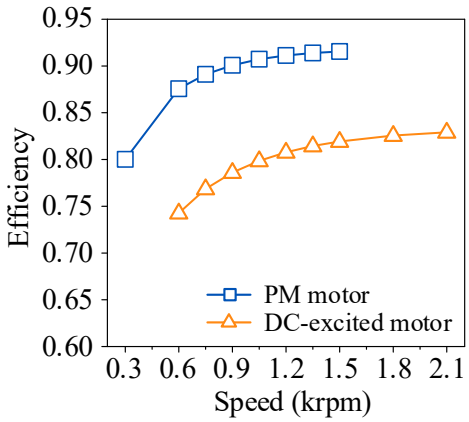

Figure12: Efficiencies under different operation speeds of the two proposed MagD motors.

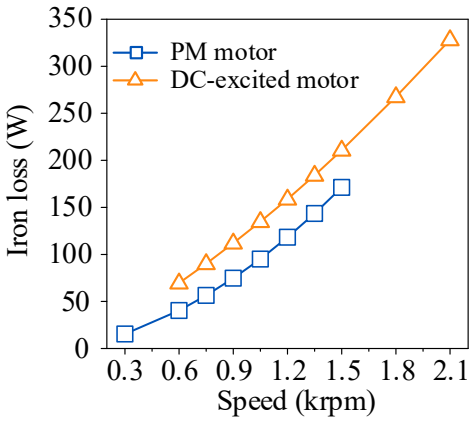

Figure13: Iron losses under different operation speeds of the two proposed MagD motors.

A detailed comparison of the motor performances under the rated working condition is presented in Table 2. In most of the performances, the FRPM MagD motor dominates. It has a larger no-load back-EMF amplitude,

more sinusoidal no-load back-EMF waveform, larger torque with lower torque ripple, higher efficiency, larger output power, and higher torque and power density than the DC-excited FR MagD motor. It can be applied to the scenario where a high torque quality is preferred regardless of the cost and a strict cooling condition to protect the PMs from demagnetization. However, although the DC-excited motor shows inferior performances in many aspects, it has the merits of a strong ability to regulate the flux. Also, the magnetless structure frees the DC-excited motor from the risk of demagnetization. What is more, the insignificant magnetic forces between the stator and its two rotors not only alleviate the manufacturing difficulty but also reduce the maintenance burden. It suits many low-cost situations desiring a simple and robust magnetic differential.

Table 2: Motor performances comparison

Performances	FRPM MagD motor	DC-excited FR MagD motor
No-load back-EMF (Amplitude, V)	49.4	29.0
THD	4.7%	9.4%
Total torque (Nm)	23.6	11.0
Torque ripple	7.0%	15.6%
Torque density (Nm/kg)	1.49	0.86
Range of back-EMF (Amplitude, V)	[47.3, 55.1]	[0, 29.0]
Range of torque on each rotor (Nm)	[11.1, 12.2]	[0, 5.5]
No-load magnetic force on each rotor (N)	1538.6	0
Onload magnetic force on each rotor (N)	1586.2	408.5
Efficiency	90.1%	78.6%
Iron loss (W)	74.7	112.0
Output power (W)	2211.6	1035.1
Power density (W/kg)	139.6	76.9

5 Conclusion

This paper provides a comprehensive comparison between a FRPM motor and a DC-excited FR motor with MagD application for EVs. The structural design and the operation principles of the two proposed MagD motors are demonstrated minutely. Based on 3D FEA using the software JMAG, the no-load back-EMF, the electromagnetic torque, the flux regulation ability, and the motor efficiency and iron loss, as well as the magnetic force between stator and rotors, are all investigated in detail. Through the comparison, it can be found that both motors can work properly as the magnetic differential. The FRPM motor is preferred in scenarios where higher torque density and high efficiency are required. However, it lacks efficiency in regulating the flux and adds some burden to the motor structure and cost due to the PMs. To prevent the PMs from demagnetization, the current density of the MC windings should be limited, and the cooling condition needs to keep the operating temperature not too high. On the other hand, however, the DC-excited FR motor can relieve the aforementioned concerns for the FRPM motor. It is free from the risk of demagnetization and easy to build. In addition, the simple structure of the DC-excited motor cuts down the cost and the maintenance burden. And it can efficiently control the flux due to the DC windings. Nevertheless, it cannot perform as well as its PM counterpart, neither the torque density nor the efficiency.

Acknowledgments

This work was supported by a grant (Project No. 17204021) from the Hong Kong Research Grants Council, Hong Kong Special Administrative Region, China.

References

[1] W. Liu, T. Placke and K. T. Chau, *Overview of batteries and battery management for electric vehicles,* Energy Reports, ISSN 2352-4847, 8(2022), 4058-4084

[2] W. Liu, K. T. Chau, H. Wang and T. Yang, *Long-range wireless power drive using magnetic extender,* IEEE Transactions on Transportation Electrification, ISSN 2332-7782, 9(2022), 1897-1909

[3] C. Liu, J. Zhong and K. T. Chau, *A novel flux-controllable vernier permanent-magnet machine,* IEEE Transactions on Magnetics, ISSN 1941-0069, 47(2011), 4238-4241

[4] J. Li and K. T. Chau, *Performance and cost comparison of permanent-magnet vernier machines*, IEEE Transactions on Applied Superconductivity, ISSN 1558-2515, 22(2012), 1-4

[5] S. Jia, R. Qu and J. Li, *Analysis of the power factor of stator DC-excited vernier reluctance machines,* IEEE Transactions on Magnetics, ISSN 1941-0069, 51(2015), 1-4

[6] L. Cao, Y. Zuo, H. Chen, S. Xie, B. S. Han, C. C. Hoang and C. H. T. Lee, *Quantitative comparison on permanent-magnet vernier machines with improved flux modulation effect for automatic guided vehicles,* IEEE Transactions on Vehicular Technology, ISSN 1939-9359, 71(2022), 11367-11378

[7] K. T. Chau, Y. B. Li, J. Z. Jiang and C. Liu, *Design and analysis of a stator-doubly-fed doubly-salient permanent-magnet machine for automotive engines*, IEEE Transactions on Magnetics, ISSN 1941-0069, 42(2006), 3470-3472

[8] Y. Gong, K. T. Chau, J. Z. Jiang, C. Yu and W. Li, *Design of doubly salient permanent magnet motors with minimum torque ripple*, IEEE Transactions on Magnetics, ISSN 1941-0069, 42(2009), 4704-4707

[9] M. Cheng, F. Yu, K. T. Chau, and W. Hua, *Dynamic performance evaluation of a nine-phase flux-switching permanent magnet motor drive with model predictive control*, IEEE Transactions on Industrial Electronics, ISSN 1557-9948, 63(2016), 4539-4549

[10] Y. Du, F. Xiao, W. Hua, X. Zhu, M. Cheng, L. Quan, K. T. Chau, *Comparison of flux-switching PM motors with different winding configurations using magnetic gearing principle*, IEEE Transactions on Magnetics, ISSN 1941-0069, 52(2016), 1-8

[11] H. Li, Z. Q. Zhu and H. Hua, *Comparative analysis of flux reversal permanent magnet machines with toroidal and concentrated windings,* IEEE Transactions on Industrial Electronics, ISSN 1557-9948, 67(2020), 5278-5290

[12] Y. Tang, J. J. H. Paulides and E. A. Lomonova, *Winding topologies of flux-switching motors for in-wheel traction,* COMPEL: The International Journal for Computation and Mathematics in Electrical and Electronic Engineering, ISSN 0332-1649, 34(2015), 32-45

[13] X. Wang, Y. Fan, C. Yang, Z. Wu and C. H. T. Lee, *Multi-objective optimization framework of a radial-axial hybrid excitation machine for electric vehicles,* IEEE Transactions on Vehicular Technology, ISSN 1939-9359, 72(2023), 1638-1648

[14] L. Jian, K. T. Chau, Y. Gong, J. Z. Jiang, C. Yu and W. Li, *Comparison of coaxial magnetic gears with different topologies*, IEEE Transactions on Magnetics, ISSN 1941-0069, 45(2009), 4526-4529

[15] L. Cao, K. T. Chau, C. H. T. Lee, W. Li and H. Fan, *Design and analysis of electromagnetic gears with variable gear ratios,* IEEE Transactions on Magnetics, ISSN 1941-0069, 53(2017), 1-6

[16] O. P. Adeleke, Y. Li, Q. Chen, W. Zhou, X. Xu and X. Cui, *Torque distribution based on dynamic programming algorithm for four in-wheel motor drive electric vehicle considering energy efficiency optimization,* World Electric Vehicle Journal, ISSN 2032-6653, 13(2022), 181

[17] A. Gago-Calderón, L. Clavero-Ordóñez, J. R. Andrés-Díaz and J. Fernández-Ramos, *Hardware architecture and configuration parameters of a low weight electronic differential for light electric vehicles with two independent wheel drive to minimize slippage,* World Electric Vehicle Journal, ISSN 2032-6653, 10(2019), 23

[18] W. Zhang, Z. Liu and Q. Chen, *Electronic differential system based on adaptive SMC combined with QP for 4WID electric vehicles,* World Electric Vehicle Journal, ISSN 2032-6653, 12(2021), 126

[19] T. Yang, K. T. Chau, T. W. Ching, H. Zhao and H. Wang, *A magnetic-differential double-rotor flux-reversal permanent-magnet motor for electric vehicles,* 2021 24th International Conference on Electrical Machines and Systems (ICEMS), ISSN 2642-5513, 2021, 1228-1232

[20] L. Cao, K. T. Chau, C. H. T. Lee and H. Wang, *A double-rotor flux-switching permanent-magnet motor for electric vehicles with magnetic differential,* IEEE Transactions on Industrial Electronics, ISSN 1557-9948, 68(2021), 1004-1015

[21] T. Yang, K. T. Chau, W. Liu, T. W. Ching and L. Cao, *Comparative analysis and design of double-rotor stator-permanent-magnet motors with magnetic-differential application for electric vehicles,* World Electric Vehicle Journal, ISSN 2032-6653, 13(2022), 199

[22] F. Giulii Capponi, G. De Donato and F. Caricchi, Recent advances in axial-flux permanent-magnet machine technology, IEEE Transactions on Industry Applications, ISSN 1939-9367, 48(2012), 2190-2205.

[23] L. Wang, *Static eccentricity fault analysis of surface-mounted permanent magnet electromotor with skewed slots based on 2D FEA*, World Electric Vehicle Journal, ISSN 2032-6653, 12(2021), 176

[24] H. Chuan, J. K. H. Shek, *Reducing unbalanced magnetic pull of an induction machine through active control*, 8th IET International Conference on Power Electronics, Machines and Drives (PEMD 2016), 2016,1-6

Presenter Biography

Tengbo Yang received the B.Eng. degree in electronic information engineering from Zhejiang University, Hangzhou, China, in 2019. He is currently working toward the Ph.D. degree in electrical and electronic engineering with The University of Hong Kong, Pokfulam, Hong Kong. He received the Hong Kong Ph.D. Fellowship in 2019 to support his Ph.D. study. His research interests include electric machines and drives, electric vehicle technologies, and magnetic gears.